Molecular Biology of the Cell
Vol. 20, 1763–1771, March 15, 2009

Caveolin-2 Is Required for Apical Lipid Trafficking and Suppresses Basolateral Recycling Defects in the Intestine of *Caenorhabditis elegans*

Scott Parker,*† Denise S. Walker,†‡ Sung Ly, and Howard A. Baylis

Department of Zoology, University of Cambridge, Downing Street, Cambridge, CB2 3EJ, United Kingdom

Submitted August 14, 2008; Revised December 8, 2008; Accepted January 13, 2009
Monitoring Editor: Jennifer Lippincott-Schwartz

Caveolins are plasma membrane–associated proteins that colocalize with, and stabilize caveolae. Their functions remain unclear although they are known to be involved in specific events in cell signaling and endocytosis. *Caenorhabditis elegans* encodes two caveolin genes, *cav-1* and *cav-2*. We show that *cav-2* is expressed in the intestine where it is localized to the apical membrane and in intracellular bodies. Using the styryl dye FM4-64 and BODIPY-labeled lactosylceramide, we show that the intestinal cells of *cav-2* animals are defective in the apical uptake of lipid markers. These results suggest parallels with the function of caveolins in lipid homeostasis in mammals. We also show that CAV-2 depletion suppresses the abnormal accumulation of vacuoles that result from defective basolateral recycling in *rme-1* and *rab-10* mutants. Analysis of fluorescent markers of basolateral endocytosis and recycling suggest that endocytosis is normal in *cav-2* mutants and thus, that the suppression of basolateral recycling defects in *cav-2* mutants is due to changes in intracellular trafficking pathways. Finally, *cav-2* mutants also have abnormal trafficking of yolk proteins. Taken together, these data indicate that caveolin-2 is an integral component of the trafficking network in the intestinal cells of *C. elegans*.

INTRODUCTION

Caveolae are 50–100-nm invaginations located on the plasma membrane of many cell types (Anderson, 1998). They are enriched in lipid raft–associated molecules: cholesterol, sphingolipids, glycosphingolipids, and many signaling and receptor proteins. Although identified more than 50 years ago, their functions have remained elusive. However, they are known to play roles in specific cell-signaling processes, and it is clear that endocytosis through caveolae is an important clathrin-independent endocytic pathway (Parton and Richards, 2003; Parton and Simons, 2007). A range of molecules including glycosphingolipids, glycosylphosphatidylinositol (GPI)-anchored proteins, cholera toxin B, and SV40 virus have been shown to traffic through caveolae-dependent endocytosis pathways (see Marsh and Helenius, 2006; Mayor and Pagano, 2007; Parton and Simons, 2007 for reviews).

Caveolae require caveolin proteins for formation so that depletion of caveolins results in loss of morphologically detectable caveolae (Drab *et al.*, 2001; Galbiati *et al.*, 2001). Furthermore, introduction of caveolin into cells that do not produce caveolae stimulates caveolar biogenesis (Lipardi *et al.*, 1998). The majority of caveolin appears to traffic to the plasma membrane and is relatively immobile; however, internal caveolin-containing structures, named caveosomes, have been visualized (Parton and Simons, 2007) and appear to be an integral part of the caveolin-dependent endocytic machinery (Nichols, 2003). Mammalian cells have three caveolin subtypes: caveolin 1 is widely expressed, but is found at particularly high levels in adipocytes, endothelial cells, and fibroblasts. Caveolin 2 interacts with caveolin 1, whereas caveolin 3 is expressed in myocytes only. Caveolin knockout mice show a range of physiological defects (Le Lay and Kurzchalia, 2005). These include defects in lipid homeostasis (Cohen *et al.*, 2004a; Le Lay and Kurzchalia, 2005; Martin and Parton, 2005; Parton and Simons, 2007). Central to the defects in lipid homeostasis is the role of caveolin-1 in endocytosis in adipocytes (Cohen *et al.*, 2004b; Martin and Parton, 2005; Le Lay *et al.*, 2006). Mutations in caveolin-1 have also been shown to be associated with the rare lipodystrophies: Berardinelli-Seip congenital lipodystrophy (OMIM:269700) and an atypical partial lipodystrophy and hypertriglyceridemia (Cao *et al.*, 2008; Kim *et al.*, 2008a). Caveolin-1 is also required for liver regeneration (Fernandez *et al.*, 2006; Frank and Lisanti, 2007).

Caenorhabditis elegans has two caveolin genes; *cav-1* and *cav-2* (Tang *et al.*, 1997). *cav-1* has been implicated in meiotic progression in the germ line (Scheel *et al.*, 1999) and in neurotransmission at the neuromuscular junction (Parker *et al.*, 2007). *cav-1* is widely expressed in embryos but gradually develops a more restricted pattern of expression so that in late larval and adult animals it is restricted to the neuromuscular system (Scheel *et al.*, 1999; Parker *et al.*, 2007) and germ line (Scheel *et al.*, 1999). The behavior of CAV-1 in the germ line and embryos is highly dynamic (Sato *et al.*, 2006). Phylogenetic analysis and expression studies of CAV-1 and CAV-1-mammalian caveolin hybrids in mammalian cells suggest that CAV-1 does not induce caveola biogenesis (Kirkham *et al.*, 2008) and so may have a different role to mammalian caveolins. The function of CAV-2 has not previously been investigated.

This article was published online ahead of print in *MBC in Press* (http://www.molbiolcell.org/cgi/doi/10.1091/mbc.E08–08–0837) on January 21, 2009.

† These authors contributed equally to this work.

Present addresses: *Saint Louis University Medical School, St. Louis, MO 63104; ‡MRC Laboratory of Molecular Biology, Hills Road, Cambridge CB2 0QH, United Kingdom.

Address correspondence to: Howard A. Baylis (hab@mole.bio.cam.ac.uk).

© 2009 by The American Society for Cell Biology

In this work we show that *cav-2* is expressed and functions in the intestine of *C. elegans*. The intestine of *C. elegans* consists of a single layer of 20 polarized epithelial cells arranged as a tube. The apical surface of the cell is shaped into microvilli and forms the barrier with the lumen of the gut, whereas the basolateral surface is in contact with the pseudocoelomic space (body cavity; McGhee, 2007). Recent work using genetic and in vivo approaches has led to the development of the *C. elegans* intestine as a system for the study of trafficking (Fares and Grant, 2002; Grant and Sato, 2006). Grant *et al.* (2001) showed that exposure of the apical surface to lipid markers, such as FM4-64, and fluid-phase markers, such as Texas Red-BSA, results in accumulation of the markers in gut granules. Application of FM4-64 to the basolateral membrane has the same result, but basolaterally applied fluid-phase markers, such as Texas Red-BSA or ssGFP (GFP secreted into the body cavity; Fares and Greenwald, 2001b), undergo recycling. It has been shown that both RME-1 and RAB-10 are required for this fluid-phase recycling in the *C. elegans* intestine (Grant *et al.*, 2001; Chen *et al.*, 2006). RME-1, an EH domain protein, is required in a range of tissues for proper endocytosis, but mutations in the small GTPase RAB-10 cause gut-specific defects in recycling. In both cases the result of these defects is the accumulation of enlarged endocytic vesicles in the intestinal cells (Grant *et al.*, 2001; Chen *et al.*, 2006).

Here we report that depletion of CAV-2 results in reduced transport of lipid markers from the apical side of the intestine. We show that depletion of *cav-2* suppresses the vacuolar phenotype caused by defective basolateral fluid-phase recycling in *rme-1* and *rab-10* mutants. Curiously, *cav-2* mutants do not have any apparent defects in the trafficking of a variety of markers for basolateral endocytosis, but *cav-2* depletion does restore normal trafficking of these markers in *rme-1* mutants.

MATERIALS AND METHODS

C. elegans *Strains and General Phenotypic Analysis*

Maintenance, culture, and genetic manipulation of *C. elegans* were performed using standard methods (Lewis and Fleming, 1995). A list of strains used in this work is given in Supplementary Table S1. Defecation cycle length was measured as described in Kwan *et al.* (2008). Ten worms were scored for each strain. For brood-size assays, NGM plates were seeded with a 1-cm "patch" of *Escherichia coli* OP50. An individual L4 was picked to a single plate and then picked to a fresh patch plate every 12 h for 100 h. The number of live eggs laid on each plate was counted. Ten worms were scored for each strain. To quantify gut vacuoles, worms were anesthetized in 0.02% tricaine, 0.001% levamisole. Gut vacuoles were scored using differential interference contrast (DIC) optics on a Zeiss Axioskop upright microscope (Welwyn Garden City, UK). Fifty worms of each strain were scored.

Plasmids, Fluorescent Protein Reporter Constructs, and Transgenic Strains

CAV-2::GFP fusion proteins were generated with green fluorescent protein (GFP) inserted close to the 5′ or 3′ end of the gene to give N and C terminal fusions, respectively. Constructs included ca. 4 kb of DNA upstream of the ATG start (the forward primer was SP650: cgatctactatgcctccaatggg) and 2 kb of DNA downstream of the stop codon (the reverse primer was SP653: cgagtgaaagcacgtgacgac). The *cav-2::gfp* transcriptional fusion was constructed with the same upstream DNA. The *cav-2::yfp* fusion used in colocalization studies contains an N terminal fusion of yellow fluorescent protein (YFP) to the full *cav-2* gene and used the same upstream and downstream regions.

rme-1 and *rme-8* fusions to cyan fluorescent protein (CFP) were generated using the PCR fusion technique (Hobert, 2002), enabling attachment of CFP to the C terminus. CFP was amplified with a 3′ untranslated region (UTR) from *let-858* using plasmid pSP002, a derivative of pHAB200 (Baylis *et al.*, 1999) containing CFP rather than GFP, as a template. *rme-1* and *rme-8* genes and their respective 5′ regulatory regions were amplified from wild-type genomic DNA, including ~1 kb of upstream sequence. The upstream region was defined by the forward primers SP1062 gtccggtggaacttatgaacaactggc and SP1294 ccaagtaggtagcttgcaactcgc for *rme-1* and *rme-8*, respectively. The reactions were mixed and amplified using nested primers to produce *rme-1::cfp* or *rme-8::cfp* fusions.

The rescuing construct containing *cav-2* driven by its own promoter (pSP040) consisted of a genomic DNA fragment amplified using the upstream and downstream oligonucleotides SP650 and SP653 described above cloned into pGEM-T (Promega, Southampton, UK).

To construct intestine specific *cav-2* clones, we used Gateway multisite technology (Invitrogen, Paisley, UK). Individual entry clones containing the *vha-6* promoter and *cav-2* cDNA were produced and then combined in a Gateway reaction into the destination vector pHP2 (H. Peterkin and H. Baylis, unpublished data). The *vha-6* promoter clone contained a fragment, similar to that previously used by Grant and colleagues (Chen *et al.*, 2006), amplified using the oligonucleotides ggggacaagtttgtacaaaaaagcaggctcgcgttcaccactcgaccaccgaac and ggggacaacttttgtatacaaagttgtttttatgggttttggtaggttttag. The *cav-2* cDNA was amplified using the oligonucleotides ggggacaactttctatacaaagttgaaaaatgactcgtcagaatacttccgaaag and ggggacaactttattatacaaagttgttaaacatgatgaatgtgtttttc.

Constructs were microinjected into N2 worms at 7 ng/μl, and stable lines were selected. Where appropriate, worms were analyzed for fluorescence using a Leica SP1 confocal microscope (Milton Keynes, UK).

rme-1 *and* cav-2 *RNA Interference*

RNA interference (RNAi) was performed by injection of double-strand RNA (dsRNA) into the animal's gonad (Fire *et al.*, 1998; Montgomery and Fire, 1998). From *cav-2* and *rme-1*, 2.4 and 1.2 kbp, respectively, were amplified using the primers SP652: atgctagcatggataaggaagatcatcac, and SP654: atgcggccgctgctccaactgagtagaagaatgg for *cav-2* and SP1027: ccaatgatcctgctcgtcgggc and SP1028: ggctgaaggctcctcctctgacag for *rme-1*. PCR products were cloned into pGEM-T (Promega), and the resulting plasmids were used as a template for transcription from the SP6 and T7 promoters using a Megascript kit (Ambion, Austin, TX). dsRNA was produced by annealing RNA from the two preparations (Hull and Timmons, 2004). The *E. coli* chloramphenicol acetyltransferase gene (*cat*) was used as a control.

Analysis of Endocytosis

Experiments using FM4-64 and labeled BSA were conducted as described by Grant *et al.* (2001). To assess uptake of lactosylceramide, animals were incubated for 2 h in 5 μM BODIPY-tagged lactosylceramide (BODIPY FL C5 LacCer; Invitrogen, Paisley, UK).

For microscopic analysis worms were anesthetized in 0.02% tricaine, 0.001% levamisole and analyzed using a Leica SP1 laser scanning confocal microscope. For the analysis of endocytic markers and to avoid autofluorescence, intestinal GFP signals were detected at 507–513 nm (Chen *et al.*, 2006). We confirmed that the contribution of autofluorescence at this wavelength in our equipment was negligible. Where appropriate (e.g., for BODIPY FL C5 LacCer staining) images were taken using identical settings, to allow direct comparison. Quantification was performed using Image J (http://rsb.info.nih.gov/ij/; NIH, Bethesda, Maryland, MD). Analysis used three regions of interest from six worms for each condition.

Immunohistochemistry

Antibodies were raised in rabbits by Covalab UK (Cambridge, United Kingdom) against two *C. elegans* CAV-2 peptides: CNTQRPPIPQYDTVD and CTPQRRSHPQYDNLD and affinity-purified. For immunocytochemistry worms were freeze-cracked and fixed in methanol and acetone (Duerr *et al.*, 1999). Primary antibodies were applied at 15 ng/μl and incubated overnight. The secondary antibody was Alexa 488 mouse anti-rabbit IgM (Molecular Probes, Eugene, OR).

RESULTS

CAV-2 Is Expressed in the Intestine

To explore the function of caveolin 2 in *C. elegans*, we first established its location in the animal. We constructed two full-length *cav-2::GFP* fusions, with *GFP* inserted close to either the N or C terminal coding region of *cav-2*. A third transcriptional fusion drove *GFP* alone under the control of the *cav-2* promoter. All three constructs were expressed in the intestine of hermaphrodite and male wild-type animals (Figure 1). We did not detect expression in any other tissues. This pattern was confirmed with an anti-CAV-2 antibody (Figure 1). Therefore, *cav-2* has a distinct expression pattern from *cav-1*, which is expressed in embryos, neurons, and body-wall muscles (Scheel *et al.*, 1999; Parker *et al.*, 2007).

The *C. elegans* intestine consists of a tube of 20 polarized epithelial cells, with a dense layer of microvilli on their apical membrane. Both *cav-2::gfp* fusion proteins localized to the apical side of the intestinal cells, very close to or within

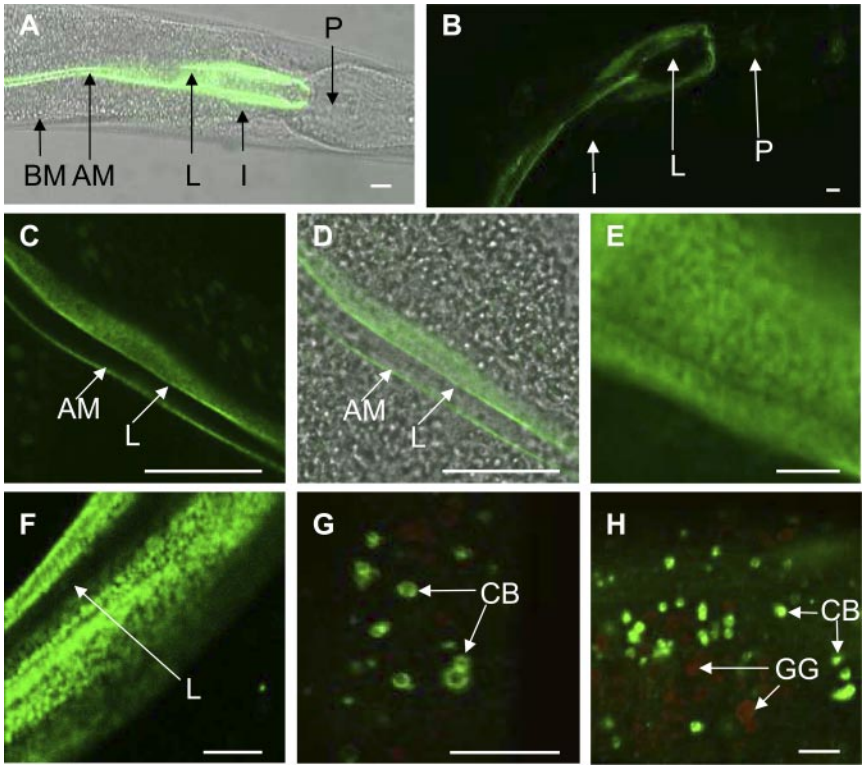

Figure 1. Caveolin-2 is located in the apical membranes of intestinal cells and in intracellular CAV-2 bodies. (A, C, and D) Confocal images of *C. elegans* carrying a *cav-2::gfp* transgene. CAV-2::GFP is expressed in the intestine (I) and is localized to the apical membrane (AM), as shown in A and at higher magnification in C and D. A and D are overlaid with transmitted light images. I, intestine; AM, apical membrane; BM, basolateral membrane; L, lumen; P, pharynx. (B) Staining with an anti-CAV-2 antibody confirms expression in the intestine. L, lumen; P, pharynx. (E and F) CAV-2 shows a punctate distribution in the apical membrane. (E) Confocal images of a section of apical membrane in CAV-2::GFP–expressing worms and (F) worms stained with an anti-CAV-2 antibody. (G and H) CAV-2 is also localized in vesicular structures (CAV-2 bodies). Confocal images of CAV-2 bodies (CB) identified by CAV-2::GFP labeling (green). Autofluorescent gut granules (GG) are shown in red. Scale bars, 10 μm.

the membrane. Expression was first detected in midstage embryos and continued thence forward. The expression at the apical membrane was highest and most evenly distributed in L1 and L2 animals. With maturation, levels of CAV-2 were highest at the anterior and posterior cells of the intestine (Figure 1). Interestingly, the labeling of the membrane was discontinuous (Figure 1). We also observed the presence of discrete, spherically shaped, CAV-2::GFP–positive vesicles (diameter, 1.6 μm; n = 30). These vesicles were most common at the posterior end of the gut and were distinct from autofluorescent gut granules (AFGGs), which are terminal endocytic lysosomes (Figure 1). We call these structures CAV-2 bodies, as their relationship to mammalian caveosomes is unknown.

cav-2 *Animals Have Reduced Fertility*

The intestine of *C. elegans* performs a range of important functions including the following: the uptake and transport of nutrients, the production and export of egg yolk proteins, and the encoding of an ultradian oscillator controlling the defecation cycle (Kimble and Sharrock, 1983; Dal Santo *et al.*, 1999; McGhee, 2007). To analyze the function of *cav-2* in the intestine, we used *cav-2* RNAi and two strains carrying putative null mutations of the *cav-2* gene: HB508, *cav-2(tm394)*, and BA1090, *cav-2(hc191)*. *cav*-2 mutants and *cav*-2(*RNAi)*-treated worms do not show any gross phenotypes. They grow at the normal rate and have normal life spans and normal defecation cycles (data not shown). However, both mutants have a slight but reproducible reduction in brood size (N2: 315 ± 8; *cav-2(hc191)*: 261 ± 23; *cav-2(tm394)*: 284 ± 28; mean ± SD). That the depletion of *cav-2*, presumably in the intestine, reduces brood size might be explained by deficiencies in nutrient uptake, trafficking, or yolk protein production.

cav-2 *Mutants Exhibit Altered Apical Trafficking*

To test whether CAV-2 depletion altered endocytosis or trafficking in the intestine, we used the fluorescent fluid and lipid-phase markers, Texas Red-BSA and FM4-64, respectively, as used by Grant and colleagues (Grant *et al.*, 2001). To follow trafficking from either side of the cell, dyes were applied to the apical (luminal) side of the intestine by feeding or to the basolateral side by microinjection into the body cavity. The anterior intestinal cells were compared. AFGGs were also visualized. Wild-type animals exposed to FM4-64 by apical or basolateral delivery rapidly endocytosed the dye and directed it to the AFGGs (Figure 2). Basolateral uptake of FM4-64 in *cav-2(tm394)* animals was normal (Figure 2), but apical uptake of FM4-64 in these animals was perturbed. Uptake is reduced by more than 50% (Figure 2O), and no or very little of the FM4-64 reached the AFGGs (Figure 2K). Any FM4-64 that was delivered to the AFGG region only stained the periphery of the granule. In contrast, wild-type animals had staining throughout the AFGGs (Figure 2, G–I). This phenotype was rescued by reintroducing a full-length wild-type copy of *cav-2* into *cav-2(tm394)* animals (HB572; Figure 2M). To confirm that this phenotype resulted from defective uptake in the intestine, we rescued *cav-2* using an intestine specific promoter (*vha-6p*; Chen *et al.*, 2006). Animals rescued in this way have normal uptake of FM4-64 (Figure 2, N and O). Thus, *cav-2* mutants have limited ability for uptake of FM4-64 at apical membranes and process the small amount of internalized dye differently to N2s.

To observe fluid-phase trafficking, we performed similar experiments using Texas Red-BSA. We did not detect any differences between wild-type and *cav-2(lf)* animals. To further explore fluid-phase uptake from the body cavity, we used a strain (GS1912) in which GFP (referred to as ssGFP) is secreted into the body cavity of worms from body wall

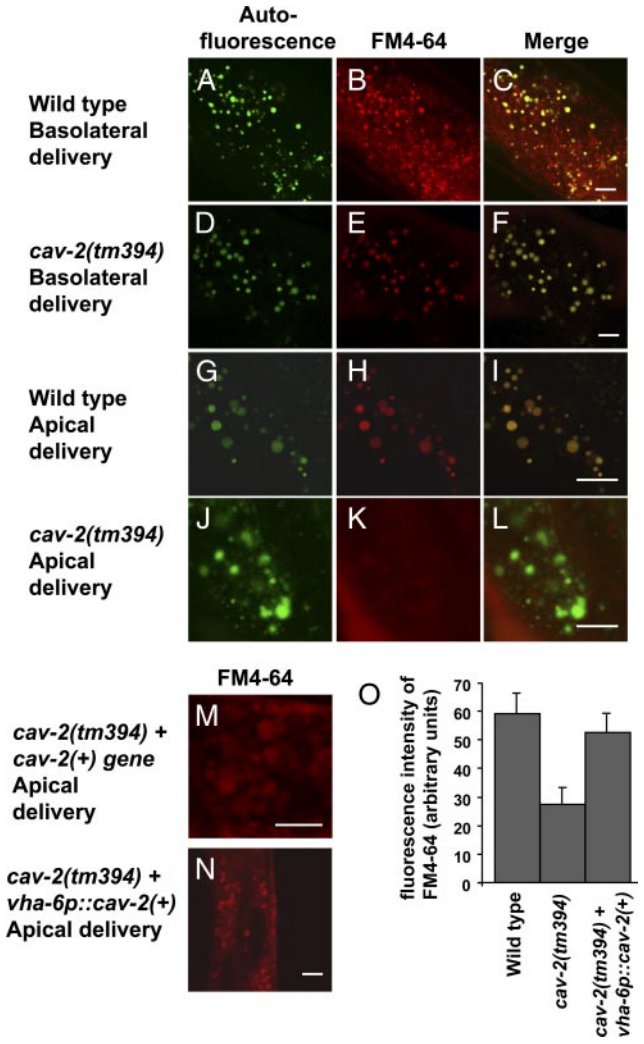

Figure 2. *cav-2* mutants show defective accumulation of the lipid trafficking indicator FM4-64. Autofluorescence, primarily associated with gut granules, is shown in green, and FM4-64 is shown in red. Merged images reveal colocalization. (A–C) Wild-type (N2) animals exposed to basolateral FM4-64 show colocalization of FM4-64 and autofluorescence. (D–F) *cav-2(tm394)* animals exposed to basolateral FM4-64 show normal uptake. (G–I) Wild-type animals exposed to apical FM4-64 show colocalization of FM4-64 and autofluorescence. (J–L) *cav-2(tm394)* animals exposed to apical FM4-64 take up very low levels of dye. FM4-64 is no longer apparent in autofluorescent gut granules. (M) *cav-2(tm394)* animals carrying a wild-type *cav-2* transgene exposed to apical FM4-64 show normal uptake. (N) *cav-2(tm394)* animals carrying an intestine specific *cav-2* cDNA transgene, *vha-6p::cav-2* exposed to apical FM4-64 show normal uptake. Scale bars, (A–N) 10 μm. (O) Quantification of FM4-64 fluorescence. Error bars, SD. For each strain six animals were sampled in three regions.

muscles (Fares and Greenwald, 2001a). We observed no changes in distribution of ssGFP either in the intestine (see Figure 5) or in coelomocytes (Supplementary Figure S1), another cell type used in the study of endocytosis.

To confirm that *cav-2* mutants have defects in apical trafficking, we exposed animals to BODIPY-tagged lactosylceramide (BODIPY FL C5 LacCer, Invitrogen). It has previously been shown that glycosphingolipid analogues are internalized through a predominantly caveolin-dependent route in human cells (Singh *et al.*, 2003; Mayor and Pagano, 2007; Singh *et al.*, 2007). In wild-type animals exposed to 5 μM BODIPY-LacCer for 2 h, fluorescent LacCer accumulates in a punctate pattern in the intestine. These putative vesicles do not generally overlap with AFGGs (Figure 3). In *cav-2(tm394)* animals, BODIPY-LacCer accumulation is reduced by ~70% (Figure 3). Thus *cav-2* depletion causes a specific defect in the uptake of both FM4-64 and BODIPY LacCer from the apical side of the intestine.

cav-2 *Suppresses Trafficking Defects in Mutants with Basolateral Recycling Defects*

Our results implicate *cav-2* in trafficking events in the intestine. To investigate if *cav-2* plays a wider role in intestinal trafficking, we tested for interactions with a known intestinal trafficking gene, *rme-1*. RME-1 is strongly implicated in endocytic recycling and *rme-1* mutants develop large intestinal vacuoles (Grant *et al.*, 2001). We tested whether *rme-1* and *cav-2* interact in the intestine. We found that *cav-2* loss-of-function mutations resulted in a marked reduction in the number and size of vacuoles resulting from *rme-1* RNAi (Figure 4). Similarly, we made a double homozygous strain carrying cav-*2(tm394)* and *rme-1(b1045)* (HB570), and these worms exhibited reduced vacuole numbers compared with *rme-1(b1045)* alone. Rescue of the *cav-2* deficiency in *cav-2(tm394); rme-1(b1045)* double mutants, by expression of a wild-type *cav-2* transgene, or intestine-specific expression of *cav-2* from a *vha-6p::cav-2(+)* transgene resulted in an increase in vacuole numbers (Figure 4). Thus, depletion of *cav-2* can significantly rescue the vacuole phenotype that results from *rme-1* depletion. In contrast to *cav-2* mutants, *rme-1* mutants show normal accumulation of FM4-64 from both the apical and basolateral membrane (Grant *et al.*, 2001). However, *rme-1(b1045);cav-2(tm394)* worms show similarly reduced levels of FM4-64 uptake from the apical membrane as do *cav-2(tm394)* worms (Figure 2; data not shown). So although *cav-2* mutations rescue the *rme-1* defect, *rme-1* mutations do not rescue the *cav-2* lipid-uptake defect. *rme-1* mutants also have defects in yolk protein uptake by oocytes (Grant *et al.*, 2001). Depletion of *cav-2* by RNAi did not suppress this defect (Supplementary Figure S2).

Because *cav-2* and *rme-1* interact, we tested whether the two proteins colocalize by using rescuing *rme-1::cfp* (see Supplementary Figure S3) and *cav-2::yfp* constructs. RME-1::CFP was localized to the basolateral membrane and distinct internalized vesicles, which are clearly separate from CAV-2::YFP labeling (Figure 4, C and D). We cannot rule out low level or transient colocalization between these two proteins. The distribution of neither gene is changed by loss of the other (data not shown).

To test whether the ability of *cav-2(lf)* to suppress defects in basolateral recycling was specific to *rme-1*, we performed *cav-2(RNAi)* on *rab-10(q373)* mutant animals. *rab-10* animals also have defects in basolateral endocytic recycling (Chen *et al.*, 2006) and also accumulate large fluid filled vesicles. Unlike *rme-1*, *rab-10* mutants only have observable defects in the intestine. We found that *cav-2(RNAi)* was also able to suppress the number of vacuoles in *rab-10(q373)* animals (Figure 4E) confirming that depletion of *cav-2* suppresses the abnormal formation of enlarged basolateral endosomes.

cav-2 *Animals Have Normal Trafficking of Basolateral Transmembrane Cargoes*

The ability of *cav-2(lf)* to rescue the accumulation of abnormal recycling endosomes in *rme-1* mutants might be explained by defects in basolateral endocytosis or by subsequent altered trafficking of endocytosed cargoes. We observed no changes in the distribution of FM4-64, Texas

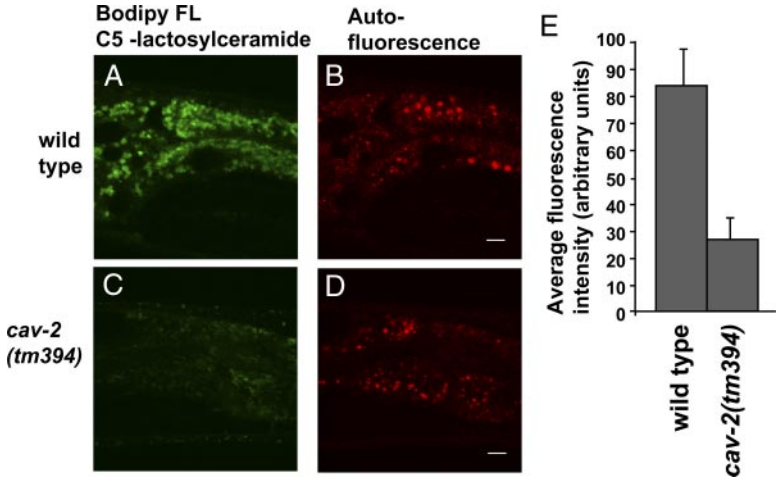

Figure 3. *cav-2* mutants show defective accumulation of fluorescently labeled lactosylceramide. (A) Wild-type worms show substantial uptake of BODIPY FL C5 LacCer into small vesicles of an unknown nature. (B) Autofluorescence for comparison with A. (C) *cav-2(tm394)* animals show significantly reduced BODIPY FL C5 LacCer uptake. (D) Autofluorescence for comparison with C. Images were collected using identical confocal settings. Images are representative examples of >20 worms. Scale bars, 10 μm. (E) Quantification of BODIPY FL C5 LacCer fluorescence. Error bars, SD. For each strain six animals were sampled in three regions.

Red BSA, or ssGFP on exposure of the basolateral membrane of the intestine, although it should be noted that both Texas Red BSA and ssGFP are hard to detect internally in normal animals. We therefore tested whether *cav-2* depletion altered trafficking of three cargo proteins fused to GFP that were previously developed and utilized by Grant and colleagues (Chen *et al.*, 2006). They are human transferrin receptor (hTfR-GFP), which has been used as a marker of clathrin-dependent uptake and of subsequent *rme-1*–mediated recycling (Chen *et al.*, 2006 and references therein); human IL-2

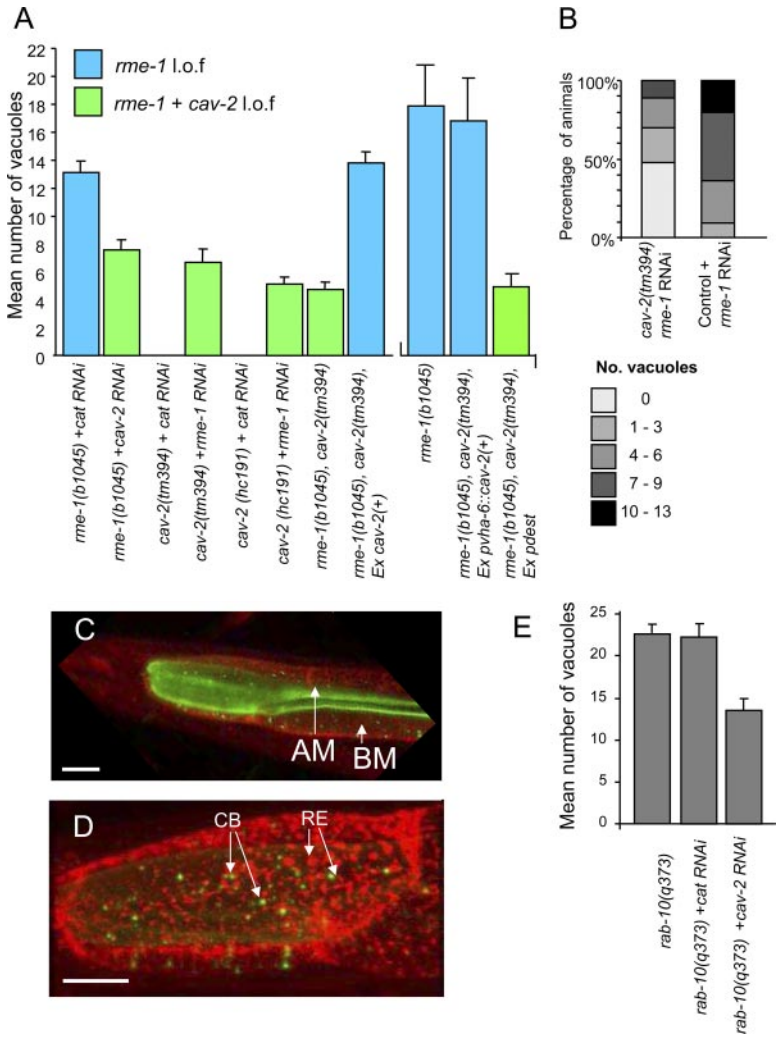

Figure 4. Reduction of *cav-2* function alleviates the vacuolar phenotype associated with defects in trafficking caused by *rme-1* and *rab-10* reduction. (A) Knockdown or knockout of *cav-2* reduces vacuole formation in *rme-1* loss-of-function animals. The mean number of vacuoles in animals of the indicated genotype is shown. *rme-1* function was reduced by mutation *rme-1(b1045)* or RNAi. Similarly, *cav-2* function was reduced by mutation *tm394* or *hc191* or by RNAi. Results for *rme-1* loss-of-function alone are shown in blue, whereas those for *rme-1* and *cav-2* loss of function are shown in green. *tm394* or *hc191* alone do not cause a phenotype. Expression of a wild-type *cav-2* transgene (*Ex cav-2*) or an intestinal specific *cav-2* transgene (*vha6p::cav-2(+)*) in the *cav-2; rme-1* double mutants restores vacuole levels to the normal *rme-1* level. Error bars, SEM. (B) Detailed breakdown of vacuolar number. *rme-1* was knocked down by RNAi in strains that carried YP-170::GFP with or without a *cav-2* mutation (HB523 and DH1033, respectively). (C and D) CAV-2 and RME-1 are present on different subcellular structures. Confocal images of a section of intestine (C) and a single intestinal cell (D) in animals carrying *cav-2::yfp* (green) and *rme-1::cfp* (red). CAV-2 labels the apical membrane (AM) and sparse CAV-2 bodies (CB), whereas RME-1 primarily labels the basolateral membrane (BM) and putative recycling endosomes (RE). Scale bars, 20 μm. (E) Reduction of *cav-2* function suppresses the vacuolar phenotype caused by *rab-10* loss of function. The mean number of vacuoles in animals of the indicated genotype is shown. Error bars, SEM.

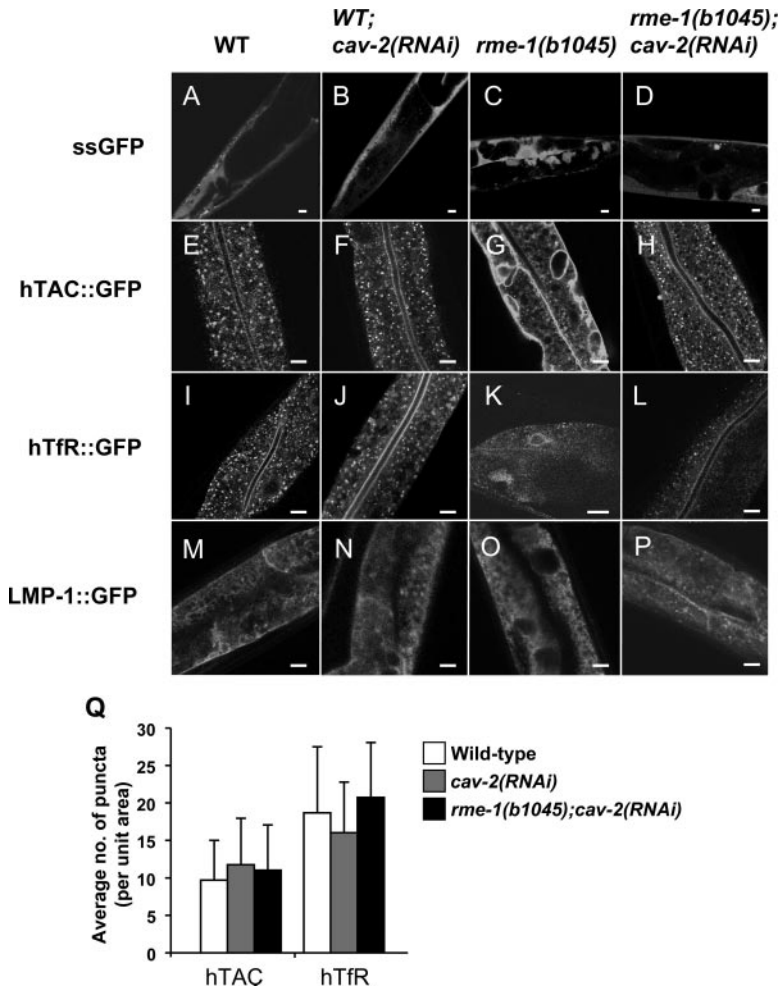

Figure 5. *cav-2* depletion restores the trafficking of endocytic markers in *rme-1* mutants to normal. (A–D) Confocal images showing the distribution of secreted GFP (ssGFP). *rme-1* mutants cause the accumulation of large ssGFP-filled vesicles in the intestine (C), but these are not observed when *cav-2* is depleted in *rme-1* animals (D). *cav-2(RNAi)* animals show normal ssGFP localization (B). (E–P) Distribution of hTAC::GFP (E–H), hTfR::GFP (I–L), and LMP-1::GFP (M–P). Scale bars,10 μm. (Q) Quantification of the number of endocytosis marker-GFP puncta. *rme-1(b1045)* animals were not quantified as the distribution of the marker is substantially different to the other samples. Error bars, SD. For each strain six animals were sampled in three regions. Each of the three markers has a characteristic pattern in the intestine of wild-type animals (E, I, and M). Depletion of *cav-2* does not alter this pattern (F, J, N, and Q). However depletion of *rme-1* produces characteristic changes in the distribution of each marker (Chen *et al.*, 2006). These changes are suppressed by the depletion of *cav-2* in the *rme-1(b1045)* animals (H, L, P, and Q).

receptor (hTAC-GFP), a marker for clathrin-independent uptake and also subsequent *rme-1*–mediated recycling (Chen *et al.*, 2006 and references therein); and *C. elegans* LMP-1 (LMP-1-GFP), which is the worm ortholog of CD63/LAMP that labels endocytic compartments within the intestine (Hermann *et al.*, 2005; Chen *et al.*, 2006). In each case we observed distributions similar to those reported by Chen *et al.* (2006) in wild-type animals (Figure 5). We then examined the distribution in animals in which *cav-2* was depleted. The number of GFP puncta was quantified for the hTfR and hTAC cargoes (Figure 5Q). In each case the distribution and number of puncta was unaltered (Figure 5), suggesting that both clathrin-dependent and -independent basolateral uptake and recycling are unaltered in *cav-2(lf)* animals.

cav-2 *Depletion Fully Suppresses Recycling Defects in* rme-1 *Mutants*

Chen *et al.* (2006) observed redistribution of each of the markers used above in *rme-1(b1045)* animals compared with wild type. We extended our analysis to address the effect of *cav-2(RNAi)* on the distribution of the three cargo proteins in *rme-1(b1045)* animals. For each marker we observed a distribution similar to that observed by Chen *et al.* in the *rme-1(b1045)* background (Figure 5). However when we depleted *cav-2* by RNAi, the distribution of each marker was returned to the wild-type pattern (Figure 5). We also determined the number of hTAC and hTfR GFP puncta in *rme-1(b1045); cav-2(RNAi)* animals and observed no significant change in comparison to wild-type animals. Thus, depletion of *cav-2* suppresses the defects observed in *rme-1*–deficient animals.

cav-2 *Mutants Have Altered Yolk Protein Distribution*

Because *cav-2* alters trafficking in the intestine, we asked whether it could alter other aspects of intestinal function. To observe the synthesis and movement of yolk proteins (vitellogenins), we used a yolk protein-GFP fusion, YP-170::GFP (also known as VIT-2::GFP (Grant and Hirsh, 1999). This construct allows visualization of yolk protein and its export into the pseudocoelomic space for ultimate delivery to the growing oocytes (Kimble and Sharrock, 1983; Hall *et al.*, 1999). We crossed this marker into *cav-2(tm394)* worms to generate HB523. Analysis of HB523 revealed that *cav-2(lf)* resulted in an increased accumulation of YP-170::GFP in the pseudocoelom, a swollen tail phenotype, and punctate accumulations of YP-170::GFP (Figure 6). Levels of YP-170::GFP in the HB523 intestine appeared normal but less localized to the basolateral membrane compared with wild type. *cav-2* RNAi has the same effect (not shown). The level of YP-170::GFP in embryos (Figure 6, C and D) and oocytes (Supplementary Figure S2) is unaltered in *cav-2* mutants, suggesting that changes in the level of YP-170::GFP in the body cavity do not result from altered uptake into oocytes. Therefore it appears that yolk protein is being exported from the intestine in larger than normal amounts, again suggest-

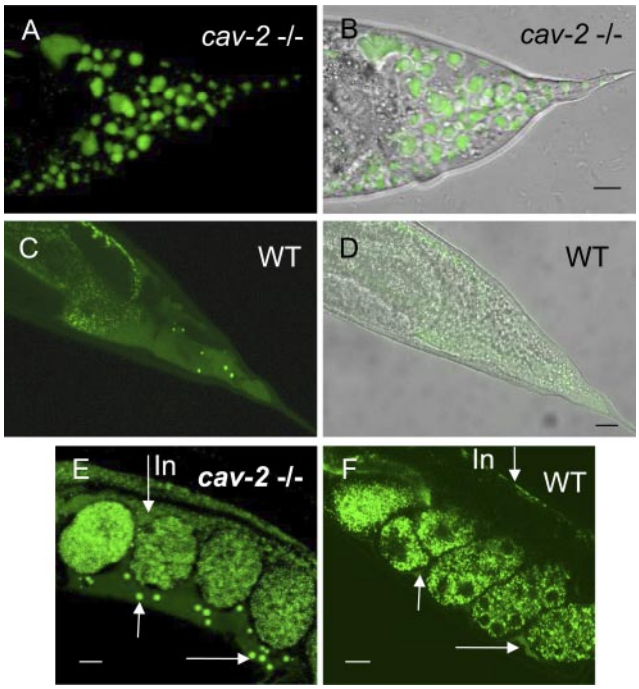

Figure 6. Trafficking of yolk protein YP-170::GFP is disrupted in *cav-2* mutants. Confocal fluorescent and transmitted light images of animals carrying the YP-170::GFP reporter fusion (Grant and Hirsh, 1999). (A and B) *cav-2(tm394)* mutant animals show accumulation of YP-170::GFP in large puncta in the pseudocoelomic space. These tend to accumulate in the tail which is often swollen. Compare the swollen tail phenotype in B and D. (C and D) In wild-type animals the YP-170::GFP is present at lower levels and tends to be diffuse with low numbers of granules (C). (E and F) *cav-2* mutants (E) and wild-type (F) animals show accumulation of YP-170::GFP in developing eggs. Scale bars, 10 μm.

ing that CAV-2 is intimately involved in basolateral trafficking in intestinal cells.

DISCUSSION

The functions of caveolins remain incompletely understood. We have shown that in *C. elegans*, *cav-2* is located in the apical membrane and in intracellular bodies in the intestine. Depletion of *cav-2* disrupts apical lipid trafficking but has no apparent effect on basolateral transport. However *cav-2* depletion is also able to suppress defects in basolateral recycling caused by depletion of either *rme-1* or *rab-10*.

C. elegans has two caveolin genes; our work and previous work has shown that these two proteins have different and largely nonoverlapping expression patterns. CAV-2 appears to be solely or primarily expressed in the intestine. CAV-1 shows a wider expression pattern in embryos and early larvae (Scheel *et al.*, 1999; Sato *et al.*, 2006; Parker *et al.*, 2007) and thus may overlap CAV-2 expression early in development. However by adulthood, *cav-1* expression is confined to the neuromuscular system and germ line. That *cav-2* also functions, primarily, in the intestine is supported by our observation of intestinal phenotypes that are rescued by intestinal expression and by the lack of any effect of *cav-2* on endocytosis in coelomocytes or oocytes. Both CAV-1 and -2 appear to be predominantly located in the membrane; however, in both cases intracellular vesicles, CAV-1 and -2 bodies, respectively, are also observed (Sato *et al.*, 2006). Sato *et al.* (2006) demonstrated that the smaller CAV-1 bodies observed in the germ line are mobile. The relationship of the CAV-2 bodies that we observed to mammalian caveosomes (Pelkmans *et al.*, 2001) is unclear. We found no colocalization of RME-1 and -8 with CAV-2 bodies and Sato *et al.* (2006) found no colocalization of EAA-1 or RME-2 with CAV-1 bodies; thus, so far no overlap between these intracellular CAV bodies and other endocytic markers in *C. elegans* has been found.

It is not known if caveolae are present in *C. elegans* because no systematic analysis of cells for the presence of caveolae has been published. The ability of CAV-2 to induce the formation of caveolae has not been tested. Kirkham *et al.*, (2008) have shown that *C. elegans* CAV-1 does not induce caveolae in mammalian cells and have used phylogenetic analysis to indentify amino acid changes that may underlie this difference (Kirkham *et al.*, 2008). In particular they identified two key regions: one involving residues 56–59 and another involving residues S104, F12, and A129 in the human caveolin 1 sequence (Supplementary Figure S4), which may determine the ability of caveolins to form caveolae. In CAV-1 the equivalent residue to P56 is A and to F124 is S. However in CAV-2 these two residues are identical to those found in humans; thus, it may be that, unlike CAV-1, CAV-2 is able to induce the formation of caveolae. Interestingly we observed a punctuate distribution of CAV-2 in the membrane using both CAV-2::GFP fusion and anti-CAV-2 antibodies.

cav-2 is expressed in the intestine of *C. elegans.* The intestine consists of a single layered tube of polarized cells (McGhee, 2007). *C. elegans* has a relatively simple anatomy, and so the intestine plays a number of roles. First, it is the primary nutritional interface with the environment, with food passing rapidly through the intestine, while nutrients are absorbed and transported. Second, it is the site of yolk protein production. Third, it is the site of a calcium-based signaling system that controls defecation, an event that occurs every 50 s (Dal Santo *et al.*, 1999). Finally, the intestine is also one of two tissues, along with the epidermis (hypodermis), that are used for fat storage (Ashrafi, 2007). Thus the intestine has large numbers of fat droplets and may be regarded as the *C. elegans* adipose tissue. We observed that *cav-2* mutants have defects in lipid trafficking from the apical membrane: the uptake of the styryl dye FM4-64 and of the BODIPY LacCer were disrupted. These results suggest that *cav-2* is required for normal lipid uptake in the intestine. This function is reminiscent of the importance of caveolin function to lipid metabolism in mammals (Cohen *et al.*, 2004b; Le Lay and Kurzchalia, 2005; Martin and Parton, 2005; Le Lay *et al.*, 2006; Parton and Simons, 2007; Garg and Agarwal, 2008; Heimerl *et al.*, 2008; Kim *et al.*, 2008b). Caveolae and CAV1 are highly concentrated in mammalian adipocytes, and it has become clear that caveolae are an important part of the trafficking system that regulates the homeostasis of lipids in adipocytes and the formation of lipid bodies. The recent discovery of mutations in CAV1 that underlie lipodystrophies emphasizes this (Cao *et al.*, 2008; Kim *et al.*, 2008a). Thus caveolins may play a conserved role in lipid homeostasis. We note that it is unlikely that CAV-2 provides the only route of lipid uptake because *cav-2* mutants grow normally. Furthermore *C. elegans* is a cholesterol auxotroph, and cholesterol depletion has the same affect on locomotion, defecation, and fecundity and is equally lethal to *cav-2* animals as it is to N2s (Parker, unpublished observation; Matyash *et al.*, 2001; Entchev and Kurzchalia, 2005). Therefore, *C. elegans* should provide a useful genetic tool for the analysis of caveolin-based lipid transport.

Depletion of *cav-2* also suppresses the vacuolated phenotype observed in *rme-1* and *rab-10* mutants. Mutations in both *rme-1* and *rab-10* result in the presence of large vesicular structures as a result of defects in basolateral recycling (Grant *et al.*, 2001; Chen *et al.*, 2006). Our understanding of endocytic recycling has advanced substantially in recent years (Maxfield and McGraw, 2004). Endocytosis at the plasma membrane causes markers (e.g., transferrin receptors) to be transported to sorting endosomes. From sorting endosomes, receptors or lipids that are to be recycled to the plasma membrane may either traffic directly to the plasma membrane or may progress to the endosome recycling compartment (ERC) from where they can traffic to the plasma membrane (Maxfield and McGraw, 2004). Genetic studies in *C. elegans* have enabled new insights into recycling mechanisms. *rab-10* and *rme-1* are components of the recycling pathway at the basolateral membrane of the intestine. Depletion of *rme-1* results in a build-up of material in ERCs, whereas depletion of *rab-10* results in increases in sorting endosome size and number; thus, the two proteins act at different steps in the pathway (Grant *et al.*, 2001; Chen *et al.*, 2006). *cav-2* mutants suppress both *rab-10* and *rme-1*. One explanation for this is that loss of *cav-2* reduces endocytosis at the basolateral membrane; however, this seems unlikely as the distribution of hTfR::GFP, hTAC::GFP, and LMP-1::GFP are all unaltered in *cav-2* mutants, suggesting that clathrin-dependent and some clathrin-independent uptake is normal. The ability of *cav-2* depletion to suppress both *rab-10* and *rme-1* may be explained if it increases trafficking directly from sorting endosomes to the plasma membrane. This would reduce build up of material in the sorting endosomes and ERC. Interestingly, Nilsson *et al.* (2008) recently identified another gene, *num-1*, which is able to suppress the effect of *rme-1* in the intestine. *num-1*, the *C. elegans* Numb ortholog is able to suppress *rme-1* mutations but not *rab-10* mutation. It also differs from *cav-2* in that it is clearly located at the basolateral membrane.

It remains unclear how depletion of *cav-2* might achieve these effects, particularly as *cav-2* appears to be primarily located at the apical membrane. However our observation that the level of yolk protein in the body cavity is increased also indicates that *cav-2* depletion has broad-ranging effects on intestinal trafficking. One possible mechanism, given our data above, is that *cav-2* depletion causes a change in the lipid composition of the cell membranes and that this in turn causes changes in trafficking throughout the cell. It is also possible that changes in apical trafficking could alter basolateral endocytosis through other mechanisms that are as yet unknown. We know very little about both apical trafficking and transcytosis in these cells. However the apparently normal distribution of, for example, hTfR::GFP, in *rme-1;cav-2* animals suggests that *cav-2* does not suppress *rme-1* through a mechanism that results in large scale relocation of endocytosed markers. Dissecting the mechanism by which *cav-2* suppresses defects in basolateral recycling should provide new insights into the molecular control of endocytosis in polarized cells.

ACKNOWLEDGMENTS

We are grateful to Barth Grant (Rutgers University, Piscataway, NJ) for many strains and advice; Jeremy Skepper (University of Cambridge, Cambridge, UK) for advice on dual color imaging; Andy Fire (Stanford University School of Medicine, CA), Mario de Bono (MRC Laboratory of Molecular Biology, Cambridge, UK), and Helen Peterkin (University of Cambridge, Cambridge, UK) for plasmids; and Hershey Monster (St. Louis University School of Medicine, St. Louis, MO) for scientific discussions. *cav-2(tm394)* was produced by the National Bioresource Project. Some strains were obtained from the Caenorhabditis Genetic Center. This work was supported by the Biotechnology and Biological Sciences Research Council (S.P., S.L.), and the Medical Research Council (MRC) (H.A.B., D.S.W., S.L.). H.A.B. was an MRC Senior Fellow.

REFERENCES

Anderson, R. G. (1998). The caveolae membrane system. Annu. Rev. Biochem. *67*, 199–225.

Ashrafi, K. (2007). Obesity and the regulation of fat metabolism (March 9), *WormBook*, ed. The *C. elegans* Research Community, WormBook, doi/10.1895/wormbook.1.13.1, http://www.wormbook.org.

Baylis, H. A., Furuichi, T., Yoshikawa, F., Mikoshiba, K., and Sattelle, D. B. (1999). Inositol 1,4,5-trisphosphate receptors are strongly expressed in the nervous system, pharynx, intestine, gonad and excretory cell of *Caenorhabditis elegans* and are encoded by a single gene (*itr-1*). J. Mol. Biol. *294*, 467–476.

Cao, H., Alston, L., Ruschman, J., and Hegele, R. A. (2008). Heterozygous CAV1 frameshift mutations (MIM 601047) in patients with atypical partial lipodystrophy and hypertriglyceridemia. Lipids Health Dis. *7*, 3.

Chen, C. C., Schweinsberg, P. J., Vashist, S., Mareiniss, D. P., Lambie, E. J., and Grant, B. D. (2006). RAB-10 is required for endocytic recycling in the *Caenorhabditis elegans* intestine. Mol. Biol. Cell *17*, 1286–1297.

Cohen, A. W., Hnasko, R., Schubert, W., and Lisanti, M. P. (2004a). Role of caveolae and caveolins in health and disease. Physiol. Rev. *84*, 1341–1379.

Cohen, A. W., Razani, B., Schubert, W., Williams, T. M., Wang, X. B., Iyengar, P., Brasaemle, D. L., Scherer, P. E., and Lisanti, M. P. (2004b). Role of caveolin-1 in the modulation of lipolysis and lipid droplet formation. Diabetes *53*, 1261–1270.

Dal Santo, P., Logan, M. A., Chisholm, A. D., and Jorgensen, E. M. (1999). The inositol trisphosphate receptor regulates a 50-second behavioral rhythm in *C. elegans*. Cell *98*, 757–767.

Drab, M., *et al.* (2001). Loss of caveolae, vascular dysfunction, and pulmonary defects in caveolin-1 gene-disrupted mice. Science *293*, 2449–2452.

Duerr, J. S., Frisby, D. L., Gaskin, J., Duke, A., Asemely, K., Huddleston, D., Eiden, L. E., and Rand, J. B. (1999). The *cat-1* gene of *Caenorhabditis elegans* encodes a vesicular monoamine transporter required for specific monoamine-dependent behaviors. J. Neurosci. *19*, 72–84.

Entchev, E. V., and Kurzchalia, T. V. (2005). Requirement of sterols in the life cycle of the nematode *Caenorhabditis elegans*. Semin. Cell Dev. Biol. *16*, 175–182.

Fares, H., and Grant, B. (2002). Deciphering endocytosis in *Caenorhabditis elegans*. Traffic *3*, 11–19.

Fares, H., and Greenwald, I. (2001a). Genetic analysis of endocytosis in *Caenorhabditis elegans*: coelomocyte uptake defective mutants. Genetics *159*, 133–145.

Fares, H., and Greenwald, I. (2001b). Regulation of endocytosis by CUP-5, the *Caenorhabditis elegans* mucolipin-1 homolog. Nat. Genet. *28*, 64–68.

Fernandez, M. A., Albor, C., Ingelmo-Torres, M., Nixon, S. J., Ferguson, C., Kurzchalia, T., Tebar, F., Enrich, C., Parton, R. G., and Pol, A. (2006). Caveolin-1 is essential for liver regeneration. Science *313*, 1628–1632.

Fire, A., Xu, S., Montgomery, M. K., Kostas, S. A., Driver, S. E., and Mello, C. C. (1998). Potent and specific genetic interference by double-stranded RNA in *Caenorhabditis elegans*. Nature *391*, 806–811.

Frank, P. G., and Lisanti, M. P. (2007). Caveolin-1 and liver regeneration: role in proliferation and lipogenesis. Cell Cycle *6*, 115–116.

Galbiati, F., Engelman, J. A., Volonte, D., Zhang, X. L., Minetti, C.Li.M., Hou, H., Jr., Kneitz, B., Edelmann, W., and Lisanti, M. P. (2001). Caveolin-3 null mice show a loss of caveolae, changes in the microdomain distribution of the dystrophin-glycoprotein complex, and t-tubule abnormalities. J. Biol. Chem. *276*, 21425–21433.

Garg, A., and Agarwal, A. K. (2008). Caveolin-1, a new locus for human lipodystrophy. J. Clin. Endocrinol. Metab. *93*, 1183–1185.

Grant, B., and Hirsh, D. (1999). Receptor-mediated endocytosis in the *Caenorhabditis elegans* oocyte. Mol. Biol. Cell *10*, 4311–4326.

Grant, B., Zhang, Y., Paupard, M. C., Lin, S. X., Hall, D. H., and Hirsh, D. (2001). Evidence that RME-1, a conserved *C. elegans* EH-domain protein, functions in endocytic recycling. Nat. Cell Biol. *3*, 573–579.

Grant, B. D., and Sato, M. (2006). Intracellular trafficking (January 21), WormBook, ed. The *C. elegans* Research Community, WormBook, doi/10.1895/wormbook.1.77.1, http://www.wormbook.org.

Hall, D. H., Winfrey, V. P., Blaeuer, G., Hoffman, L. H., Furuta, T., Rose, K. L., Hobert, O., and Greenstein, D. (1999). Ultrastructural features of the adult

hermaphrodite gonad of *Caenorhabditis elegans*: relations between the germ line and soma. Dev. Biol. *212*, 101–123.

Heimerl, S., Liebisch, G., Le Lay, S., Bottcher, A., Wiesner, P., Lindtner, S., Kurzchalia, T. V., Simons, K., and Schmitz, G. (2008). Caveolin-1 deficiency alters plasma lipid and lipoprotein profiles in mice. Biochem. Biophys. Res. Commun. *367*, 826–833.

Hermann, G. J., Schroeder, L. K., Hieb, C. A., Kershner, A. M., Rabbitts, B. M., Fonarev, P., Grant, B. D., and Priess, J. R. (2005). Genetic analysis of lysosomal trafficking in *Caenorhabditis elegans.* Mol. Biol. Cell *16*, 3273–3288.

Hobert, O. (2002). PCR fusion-based approach to create reporter gene constructs for expression analysis in transgenic *C. elegans.* Biotechniques *32*, 728–730.

Hull, D., and Timmons, L. (2004). Methods for delivery of double-stranded RNA into *Caenorhabditis elegans.* Methods Mol. Biol. *265*, 23–58.

Kim, C. A., *et al.* (2008a). Association of a homozygous nonsense caveolin-1 mutation with Berardinelli-Seip congenital lipodystrophy. J. Clin. Endocrinol. Metab. *93*, 1129–1134.

Kim, C. A., *et al.* (2008b). The absence of caveolin-1 induced by Berardinelli-Seip congenital lipodystrophy. Diabetes Metab. *34*, A14–A14.

Kimble, J., and Sharrock, W. J. (1983). Tissue-specific synthesis of yolk proteins in *Caenorhabditis elegans.* Dev. Biol. *96*, 189–196.

Kirkham, M., *et al.* (2008). Evolutionary analysis and molecular dissection of caveola biogenesis. J. Cell Sci. *121*, 2075–2086.

Kwan, C. S., Vazquez-Manrique, R. P., Ly, S., Goyal, K., and Baylis, H. A. (2008). TRPM channels are required for rhythmicity in the ultradian defecation rhythm of *C. elegans.* BMC Physiol. *8*, 11.

Le Lay, S., Hajduch, E., Lindsay, M. R., Le Liepvre, X., Thiele, C., Ferre, P., Parton, R. G., Kurzchalia, T., Simons, K., and Dugail, I. (2006). Cholesterol-induced caveolin targeting to lipid droplets in adipocytes: a role for caveolar endocytosis. Traffic *7*, 549–561.

Le Lay, S., and Kurzchalia, T. V. (2005). Getting rid of caveolins: phenotypes of caveolin-deficient animals. Biochim. Biophys. Acta *1746*, 322–333.

Lewis, J. A., and Fleming, J. T. (1995). Basic culture methods. Methods Cell Biol. *48*, 3–29.

Lipardi, C., Mora, R., Colomer, V., Paladino, S., Nitsch, L., Rodriguez-Boulan, E., and Zurzolo, C. (1998). Caveolin transfection results in caveolae formation but not apical sorting of glycosylphosphatidylinositol (GPI)-anchored proteins in epithelial cells. J. Cell Biol. *140*, 617–626.

Marsh, M., and Helenius, A. (2006). Virus entry: open sesame. Cell *124*, 729–740.

Martin, S., and Parton, R. G. (2005). Caveolin, cholesterol, and lipid bodies. Semin. Cell Dev. Biol. *16*, 163–174.

Matyash, V., Geier, C., Henske, A., Mukherjee, S., Hirsh, D., Thiele, C., Grant, B., Maxfield, F. R., and Kurzchalia, T. V. (2001). Distribution and transport of cholesterol in *Caenorhabditis elegans.* Mol. Biol. Cell *12*, 1725–1736.

Maxfield, F. R., and McGraw, T. E. (2004). Endocytic recycling. Nat. Rev. *5*, 121–132.

Mayor, S., and Pagano, R. E. (2007). Pathways of clathrin-independent endocytosis. Nat. Rev. Mol. Cell Biol. *8*, 603–612.

McGhee, J. D. (2007). The *C. elegans* intestine (March 27), WormBook, ed. The *C. elegans* Research Community, WormBook, doi/10.1895/wormbook.1.133.1, http://www.wormbook.org.

Montgomery, M. K., and Fire, A. (1998). Double-stranded RNA as a mediator in sequence-specific genetic silencing and co-suppression. Trends Genet. *14*, 255–258.

Nichols, B. (2003). Caveosomes and endocytosis of lipid rafts. J. Cell Sci. *116*, 4707–4714.

Nilsson, L., Conradt, B., Ruaud, A. F., Chen, C. C., Hatzold, J., Bessereau, J. L., Grant, B. D., and Tuck, S. (2008). *Caenorhabditis elegans num-1* negatively regulates endocytic recycling. Genetics *179*, 375–387.

Parker, S., Peterkin, H. S., and Baylis, H. A. (2007). Muscular dystrophy associated mutations in caveolin-1 induce neurotransmission and locomotion defects in *Caenorhabditis elegans.* Invert. Neurosci. *7*, 157–164.

Parton, R. G., and Richards, A. A. (2003). Lipid rafts and caveolae as portals for endocytosis: new insights and common mechanisms. Traffic *4*, 724–738.

Parton, R. G., and Simons, K. (2007). The multiple faces of caveolae. Nat. Rev. Mol. Cell Biol. *8*, 185–194.

Pelkmans, L., Kartenbeck, J., and Helenius, A. (2001). Caveolar endocytosis of simian virus 40 reveals a new two-step vesicular-transport pathway to the ER. Nat. Cell Biol. *3*, 473–483.

Sato, K., Sato, M., Audhya, A., Oegema, K., Schweinsberg, P., and Grant, B. D. (2006). Dynamic regulation of caveolin-1 trafficking in the germ line and embryo of *Caenorhabditis elegans.* Mol. Biol. Cell *17*, 3085–3094.

Scheel, J., Srinivasan, J., Honnert, U., Henske, A., and Kurzchalia, T. V. (1999). Involvement of caveolin-1 in meiotic cell-cycle progression in *Caenorhabditis elegans.* Nat. Cell Biol. *1*, 127–129.

Singh, R. D., Marks, D. L., and Pagano, R. E. (2007). Using fluorescent sphingolipid analogs to study intracellular lipid trafficking. Curr. Protocol. Cell Biol. *24*, Unit 24 21.

Singh, R. D., Puri, V., Valiyaveettil, J. T., Marks, D. L., Bittman, R., and Pagano, R. E. (2003). Selective caveolin-1-dependent endocytosis of glycosphingolipids. Mol. Biol. Cell *14*, 3254–3265.

Tang, Z., Okamoto, T., Boontrakulpoontawee, P., Katada, T., Otsuka, A. J., and Lisanti, M. P. (1997). Identification, sequence, and expression of an invertebrate caveolin gene family from the nematode *Caenorhabditis elegans.* Implications for the molecular evolution of mammalian caveolin genes. J. Biol. Chem. *272*, 2437–2445.